

## Atomic-level In situ Imaging and Spectroscopy of Interfacial Interactions during Carbon Deposition on a Ni/CeO<sub>2</sub> Catalyst

Lawrence, E.<sup>1</sup> and Crozier, P.A.<sup>1</sup>

<sup>1</sup> Arizona State University, United States

Internal reforming of hydrocarbons in solid oxide fuel cells (SOFCs) can enhance electrochemical conversion efficiencies by eliminating the need for external fuel reforming<sup>1</sup>. Long-term stability of SOFCs may be limited by carbon deposition from the fuels onto the anode catalyst, causing deactivation of the ceramic-metal composite structure. Ni/CeO<sub>2</sub>-based catalysts may inhibit carbon deposition through a process involving lattice oxygen exchange. Natural gas consists primarily of methane (CH<sub>4</sub>) but also contains several percent of higher hydrocarbons such as ethane (C<sub>2</sub>H<sub>6</sub>) and propane (C<sub>3</sub>H<sub>8</sub>), which have been shown to deposit carbon more easily than CH<sub>4</sub><sup>2</sup>. We are interested in understanding how CeO<sub>2</sub> can affect carbon deposition at the gas-solid interface by observing structural and chemical changes at the nanoscale. *In situ* environmental transmission electron microscopy (ETEM) provides the ability to observe atomic-level structural changes under simulated reaction conditions<sup>3</sup>. *In situ* electron energy-loss spectroscopy (EELS) has allowed dynamic changes in the local oxidation state of CeO<sub>2</sub> to be determined during reduction<sup>4</sup>. A fundamental study of the local structural and chemical changes occurring at Ni/CeO<sub>2</sub> interfaces under reaction conditions will elucidate the mechanisms that enable Ni/CeO<sub>2</sub>-based catalysts to inhibit carbon deposition from light hydrocarbons.

*In situ* ETEM techniques were employed to investigate the atomic-level three-phase interactions occurring at the metal-support interface during carbon deposition from C<sub>2</sub>H<sub>6</sub> and C<sub>2</sub>H<sub>4</sub> over a model Ni/CeO<sub>2</sub> catalyst<sup>5</sup>. Structural and chemical interfacial changes occurring during species-dependent carbon deposition were determined using atomic-level imaging and EELS. Figure 1 shows the structural changes that occurred during hydrocarbon exposure. During exposure to C<sub>2</sub>H<sub>4</sub>, graphite layers formed on the Ni surface. In contrast, no carbon deposition occurred and crystalline ceria became amorphous during C<sub>2</sub>H<sub>6</sub> exposure. A high-angle annular dark-field (HAADF) image of Ni/CeO<sub>2</sub> is shown in Figure 2 and insets of energy-loss spectra acquired near a Ni/CeO<sub>2</sub> interface show an intensity ratio change in the Ce M<sub>45</sub> edge during C<sub>2</sub>H<sub>6</sub> exposure, indicating the removal of oxygen. EELS linescans showed localized reduction zones in the ceria support near Ni/CeO<sub>2</sub> interfaces during C<sub>2</sub>H<sub>6</sub> exposure while less pronounced reduction zones were observed during C<sub>2</sub>H<sub>4</sub> exposure. Rapid dehydrogenation caused graphite formation to occur on Ni surfaces during C<sub>2</sub>H<sub>4</sub> exposure, whereas the metal-support interface catalyzed the oxidative dehydrogenation of C<sub>2</sub>H<sub>6</sub> and oxidized the resulting carbonaceous species during C<sub>2</sub>H<sub>6</sub> exposure. These experiments demonstrate that the ability of the interfacial sites on Ni/CeO<sub>2</sub> to inhibit carbon deposition during reforming is strongly influenced by thermodynamic and kinetic considerations which may show significant variation among different hydrocarbon species<sup>6</sup>.

### References:

- [1] Gür, T.M., *et al*, Progress in Energy and Combustion Science **54** (2016), p. 1-64.
- [2] Bierschenk, D.M., *et al*, Fuel Cells **10** (2010), p. 1129-1134.
- [3] Tao F. and Crozier P.A., Chemical Reviews **116** (2016) p. 3487-3539.
- [4] Sharma R., *et al*, Philosophical Magazine **84** (2004) p. 2731-2747.
- [5] Lawrence, E.L. and Crozier P.A., ACS Applied Nano Materials (2018) (under review).
- [6] We gratefully acknowledge support of NSF grant DMR-1308085 and ASU's John M. Cowley Center for High Resolution Electron Microscopy.

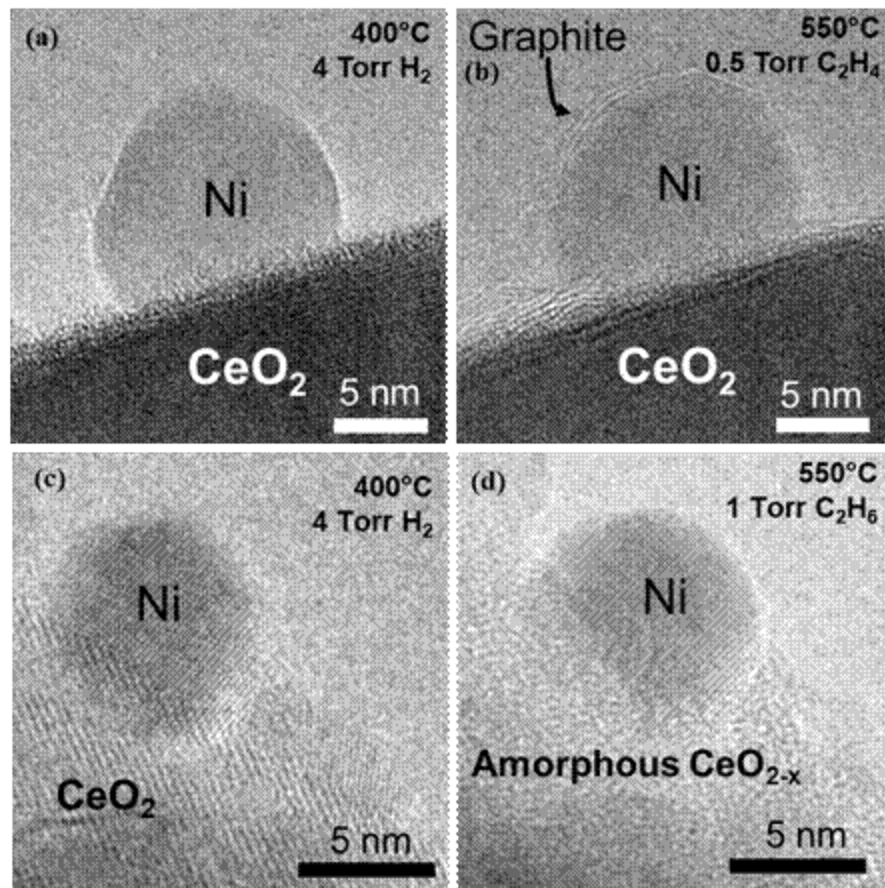


Figure 1. a) & c) Ni/CeO<sub>2</sub> at 400°C in 4 Torr H<sub>2</sub> b) Ni/CeO<sub>2</sub> in 0.5 Torr C<sub>2</sub>H<sub>4</sub> at 550°C with several graphite layers covering the Ni particle. d) Ni/CeO<sub>2</sub> in 1 Torr C<sub>2</sub>H<sub>6</sub> at 550°C. The Ni particle surface remains clear of graphite and the crystalline ceria becomes amorphous.

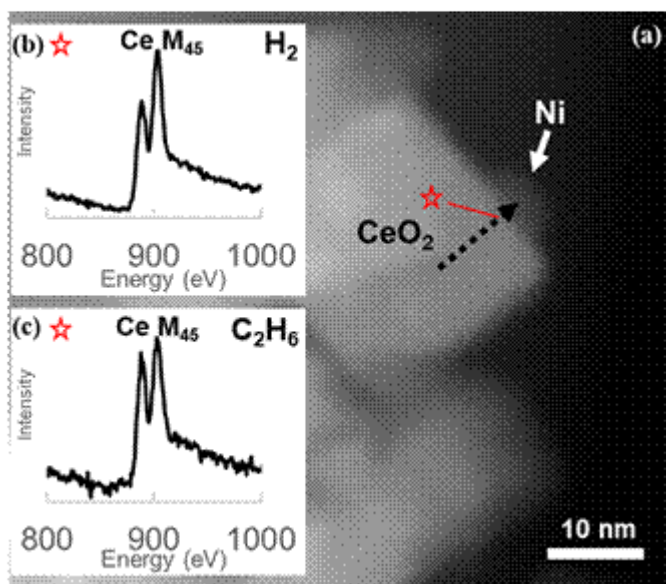


Figure 2. (a) HAADF-STEM image of Ni/CeO<sub>2</sub> catalyst. Dotted line indicates EELS linescan. Red star indicates the position on the linescan where the inserts were taken. (b) Energy-loss spectrum near Ni/CeO<sub>2</sub> interface (red star position) in 4 Torr H<sub>2</sub> at 400°C. (c) Energy-loss spectrum near Ni/CeO<sub>2</sub> interface (red star position) in 1 Torr C<sub>2</sub>H<sub>6</sub> at 550°C. Ce M<sub>45</sub> edge intensity ratio changes during C<sub>2</sub>H<sub>6</sub> exposure indicating a transition from Ce<sup>4+</sup> to Ce<sup>3+</sup>.